SNIF: A Futuristic Neutrino Probe for Undeclared Nuclear Fission Reactors

Thierry Lasserre,[1,*] Maximilien Fechner,[1] Guillaume Mention,[1] Romain Reboulleau,[2,1] Michel Cribier,[1] Alain Letourneau,[3] David Lhuillier,[3] and Jean-Luc.Sida[1]

[1] *Commissariat à l'Energie Atomique et aux Energies Alternatives, Centre de Saclay, IRFU/SPP, 91191 Gif-sur-Yvette, France*
[2] *Ecole Polytechnique, Palaiseau, France*
[3] *Commissariat à l'Energie Atomique et aux Energies Alternatives, Centre de Saclay, IRFU/SPhN, 91191 Gif-sur-Yvette, France*

(Dated: October 19, 2010)

Today reactor neutrino experiments are at the cutting edge of fundamental research in particle physics. Understanding the neutrino is far from complete, but thanks to the impressive progress in this field over the last 15 years, a few research groups are seriously considering that neutrinos could be useful for society. The International Atomic Energy Agency (IAEA) works with its Member States to promote safe, secure and peaceful nuclear technologies. In a context of international tension, neutrino detectors could help IAEA to enforce the Treaty on the Non-Proliferation of Nuclear Weapons (NPT). In this article we discuss a futuristic neutrino application to detect and localize an undeclared nuclear reactor from across borders. The SNIF[a] project propose using a few hundred thousand tons neutrino detectors to unveil clandestine fission reactors. Beyond previous studies we provide estimates of all known background sources as a function of the detector's longitude, latitude and depth, and we discuss how they impact the detectability.

PACS numbers: 95.85.Ry, 43.60.Bf, 14.60.Lm

I. NEUTRINOS AND NON PROLIFERATION

In a context of increasing carbon-free emission energy needs, civilian nuclear energy is expanding all over the world. Globalization, as well as the goal of energy independence, led to an increase of the list of countries aiming to acquire technological know-how in the field of nuclear energy. As a consequence of the spread of practical knowledge, the possibility of diverting a nuclear facility towards non-civilian use could increase in the next 50 years. The United Nations International Atomic Energy Agency (IAEA) is working to make sure that nations use nuclear energy only for peaceful purposes [1]. Beside political difficulties regarding safeguards, the efficiency of IAEA controls may be limited by monitoring techniques in the future due to the fast growth of nuclear facilities around the world. Since 2003, the Department of Safeguards of the International Atomic Agency has been evaluating the potential applicability of antineutrino detection technologies for safeguard purposes.

In 2008, a transverse working group of reactor neutrino experts from the Member States together with the IAEA Division of Technical Support (SGTS) firmly established that antineutrino detectors have unique abilities to non intrusively monitor nuclear reactor operational status, power and fissile content in real-time, from outside the reactor containment. This led to the definition of three safeguards scenarios of interest. The first two, the confirmation of the absence of unrecorded production of fissile material in declared reactors and the estimation of the total burn-up of a reactor core, are related to the so-called near-field applications with detectors located a few tens of meters from the core. The third scenario concerns clandestine or undeclared nuclear reactor detection with core-detector distances ranging from tens to hundreds of kilometers, also known as the far-field application.

As far as near-field monitoring is concerned, a few detectors specifically built for safeguards have showed robust, long term measurements of these metrics in actual installations at operating power reactors [2, 3]. Several experimental programs [6] are currently being carried out in Brazil, France, Italy, Japan, US, and Russia, guided by IAEA inputs on their needs with specific reactors. Over a longer time scale, it has been recognized that antineutrino detectors could have a considerable value in bulk process and safeguards by design approaches for new and next generation reactors.

Concerning far-field applications, preliminary discussions indicated that clandestine reactor antineutrino detection would face formidable obstacles to implementation. The purpose of this article is to address the possibility of detecting undeclared nuclear reactors across borders with very large antineutrino detectors, outlining basic principles and figures regarding the deployment of large antineutrino detectors as a safeguard tool. Such a detection possibility has already been discussed in [4, 5], using a network of gigantic water Cerenkov detectors (of 1 million tons each) being deployed below four kilometers of water in deep oceans. Our study revisits the detectability of clandestine nuclear reactors, but with a few hundreds thousand tons antineutrino detectors instead (section V).

We first review the neutrino backgrounds (section IV) to be expected in such a detector. We then establish

* Corresponding author: thierry.lasserre@cea.fr
[a] Secret Neutrino Interactions Finder

the rogue activity detection criteria in section V. In section VI we study non neutrino backgrounds in order to derive and eventually relax the minimum operation depth with respect to previous studies [5]. We also provide a method for determining the location of an undeclared reactor (section VII). We conclude by addressing the feasibility of the project within the next thirty years, discussing the detector layout (section VIII).

II. CLANDESTINE REACTORS AS ANTINEUTRINO SOURCES

A. Production of neutrinos by reactors

Fission reactors are prodigious producers of neutrinos, emitting about 10^{21} $\bar{\nu_e}$ s^{-1} per station. In modern reactors, the uranium fuel is enriched to a few percent in ^{235}U. The fission of ^{235}U produces elements which must shed neutrons to approach the valley of stability. The beta decays of these fission products produce approximately six electron antineutrinos per fission. The $\bar{\nu}_e$ spectrum above detection threshold is mainly the result of β^- decays of ^{235,238}U and ^{239,241}Pu fission products. Measurements for ^{235}U and ^{239,241}Pu and theoretical calculations for ^{238}U are used to evaluate the $\bar{\nu}_e$ spectrum [8–10]. Since ^{238}U only contributes to about 11 % of the neutrino signal, and further since the error associated with this summation method is less than 10 %, ^{238}U contributes less than 1 % to the overall uncertainty in the $\bar{\nu_e}$ flux. The overall normalization is known to about 1.4% [11] and its shape to about 2% [12]. As a nuclear reactor operates, the proportions of the fissile elements evolve with time. During a typical fuel cycle, the Pu concentrations increase so the total neutrino flux grows with time. As an approximation we use a typical averaged fuel composition during a reactor cycle corresponding to ^{235}U (55.6 %), ^{239}Pu (32.6 %), ^{238}U (7.1 %) and ^{241}Pu (4.7 %).

B. Neutrino oscillations

There is now compelling evidence for flavor conversion, also known as oscillations, of atmospheric, solar, reactor and accelerator neutrinos [16–22]. These results imply that neutrino do have non zero masses. Because of oscillations, reactor neutrino experiments measure a rate weighted by the survival probability $P(\bar{\nu_e} \to \bar{\nu_e})$ of the $\bar{\nu_e}$ emitted by nuclear power stations at a distance (L), resulting in a deviation from the $1/L^2$ dependance that would otherwise be expected.

Reactor neutrino oscillations depend on the atmospheric Δm^2_{31} and the solar Δm^2_{21} mass splittings between the three neutrino mass eigenstates, as well as the three mixing angles θ_{12}, θ_{23}, and the small, still undetermined θ_{13} [23]. In this article, we consider minimum baselines of about 100 km. Because $\Delta m^2_{sol} << \Delta m^2_{atm}$ and according to the smallness of θ_{13}, the oscillation probability can be safely approximated by:

$$1 - P(\bar{\nu_e} \to \bar{\nu_e}) = \sin^2 2\theta_{12} \cdot \sin^2 \left(1.27 \frac{\Delta m^2_{21}[eV^2] L[m]}{E_{\bar{\nu_e}}[MeV]} \right)$$

For energies above of 1.8 MeV, the survival probability could be considered as 1 for distances of 0 to several tens of kilometers. The probability then oscillates around an asymptotic value of 0.57 as the distance ranges from about 50 km to 300 km. At further distances, much larger than the 'solar-driven' oscillation length the probability is practically very close to 0.57. In this work we treat neutrino oscillation with the state-of-the-art three neutrino oscillations formula [23], but we set θ_{13} to 0 since its small value will not impact the oscillation probability for the purpose of this study.

According to the combination of MeV range energies (E) and to baselines less of than a few 10^3 kilometers the modification of the oscillation probability induced by the coherent forward scattering from matter electrons (so-called matter effect) is less than a few percent. In this work the effect is small enough to be neglected.

C. Event rate from a nuclear reactor

The mean energy release $\langle E_f \rangle$ per fission is 205 MeV. The energy weighted cross section amounts to $\langle \sigma_f \rangle = 5.8 \times 10^{-43}$ cm^2 per fission. The reactor thermal power (P_{th}) is related to the number of fissions per second (N_f) by $N_f = 6.24 \times 10^{18}\text{sec}^{-1} \cdot P_{th}[\text{MW}] / \langle E_f \rangle [\text{MeV}]$. The event rate ($R_L$) at a distance L from the source, assuming no neutrino oscillations, is then $R_L = N_f \langle \sigma_f \rangle n_p/(4\pi L^2)$, where n_p is the number of hydrogen atoms, or free protons, of the target. As an example, a reactor with a power of 100 MW$_{th}$ induces a rate of 450 events per year in a detector containing 10^{34} protons at a distance of 100 km. As explained before, neutrino oscillations will manifest themselves as a deviation from the $1/L^2$ dependance (see Figure 1).

D. Clandestine reactors

We define clandestine or rogue reactors as nuclear reactors not declared by a country to the international community (IAEA). Like regular research or power reactors they could be copious sources of neutrinos. Not benefiting from any classified information, we assume that such reactors have the same properties as regular reactors, though their nuclear thermal power is unknown. In this article we will consider that clandestine reactors may have powers between 10 MW$_{th}$ to 2 GW$_{th}$. We consider the fuel composition of clandestine reactors to be similar to the composition of commercial reactors, on average. This assumption has no strong impact on the detectability of clandestine activity since the neutrino rate depends mainly on the thermal power.

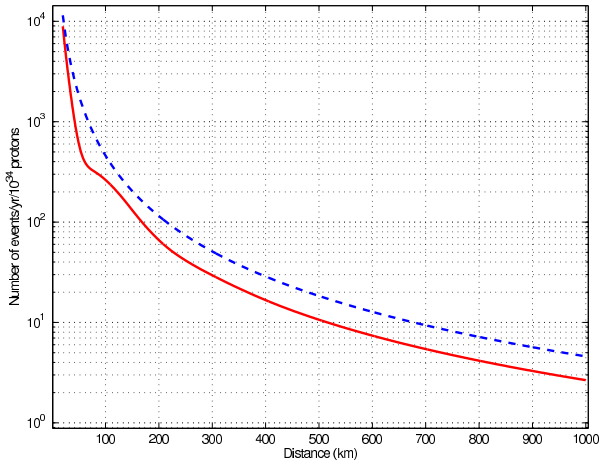

FIG. 1. Number of events detected in 1 year in a detector with 10^{34} protons, as a function of the distance from a single 100 MW reactor. The dashed line shows the variation in the absence of neutrino oscillations, while the full line shows the actual observation taking into account oscillations. From 50 km to 100 km a caracteristic 'wiggle' can be seen. Beyond 250 km, oscillations simply cause a reduction in the flux, but the $1/L^2$ dependance is restored.

III. ELECTRON ANTINEUTRINO DETECTION

Electron–antineutrinos can be detected *via* inverse beta decay on free protons: $\bar{\nu}_e + p \rightarrow e^+ + n$ for $E_{\bar{\nu}_e} > E_{thr} \sim 1.8$ MeV, and their energy is derived from the measured positron kinetic energy as $E_{\bar{\nu}_e} \simeq E_{e^+} + E_{thr}$. We call *visible energy* the energy deposited in the detector, corresponding to the $E_{vis} = E_{e^+} + 2m_e$. The inverse beta decay cross section as been precisely computed in [7]. A neutrino event is thus characterized by a prompt positron event which deposits a visible energy between 1 and 8 MeV, followed by a delayed gamma event arising from neutron capture within $\tau \sim 10 - 200\mu$sec. The minimal energy of 1 MeV of the prompt event is due to the positron annihilation in the active volume. Prompt and delayed event are spatially correlated, within< 1 m^3. They both have a β/γ-type pulse shape. This characteristic signature allows to discriminate efficiently against backgrounds. Water-Cerenkov and liquid scintillator detectors allow real-time spectroscopy of electron antineutrinos. In each case, neutrinos transfer energy to charged particles in the detector, which is converted to UV-visible light emission. Light is then collected by photomultiplier tubes covering the walls of the detector vessel. Total charge and photon arrival times allow to reconstruct the incident neutrino's energy and interaction time.

The expected neutrino rate from clandestine reactors at a few hundred kilometers is quite small, due to the weak neutrino interaction cross section. Therefore the target mass must be at least of the order of a hundred thousand tons, roughly the size of a super tanker. For fundamental research, neutrino detectors as large as 50,000 tons have been built [16]. A few projects of larger liquid scintillators detectors, like [38, 44], are currently being discussed.

In this article our reference will be a large detector, containing 10^{34} free protons. This corresponds to 138,000 tons of linearalkylbenzene (LAB) based liquid scintillator, which would be contained in a volume of 160,000 m^3. By comparison, a modern supertanker can have a capacity of over 400,000 deadweight tons. We assume that such a detector would have an 80% detection efficiency.

IV. IRREDUCIBLE NEUTRINO BACKGROUNDS

In this section we review the two largest sources of backgrounds for the search of undeclared nuclear cores: power/research reactor antineutrinos and geological antineutrinos. The geological antineutrinos background is irreducible since it originates from the β decays of radioactive elements inside the Earth crust and mantle. The antineutrino background from known reactors is mainly caused by the nuclear power stations all around the world.

A. World nuclear power stations

Clandestine reactor and commercial reactor antineutrinos are totally indistinguishable. Neutrinos from commercial plants are thus an irreducible source of background that could overwelm the clandestine signal. However this background is predictable since the IAEA can access power plant geographical coordinates, thermal power, and operating status at any time. In our simulation, we included 192 nuclear power stations (most of them having multiple units) that amount to 1139 GW$_{th}$ total power. The reactor positions were checked to a precision of one hundredth of a degree, using satellite views *via* Google Earth®. We consider that the global power is stable, though reactors will be turning on and off for refueling and maintenance. We assume that the day-by-day thermal power would be knowable by the monitoring authorities, with a 3% uncertainty. This is consistent with what present day experiments are able to achieve [30, 36].

We also assume an averaged burnup composition for all cores, with a corresponding 3% systematic uncertainty. It turns out that most of the commercial nuclear power stations are located in the northern hemisphere, mainly belonging to developed countries, especially the United States of America, Europe, and Japan. These three clusters gather more than 85% of the total world nuclear power budget. Only four power stations are present in the southern hemisphere, in Argentina, Brazil, and South Africa, amounting to only 14 GW$_{th}$. This asymmetry will play an important role in the sensitivity of the neutrino method. The total power produced by

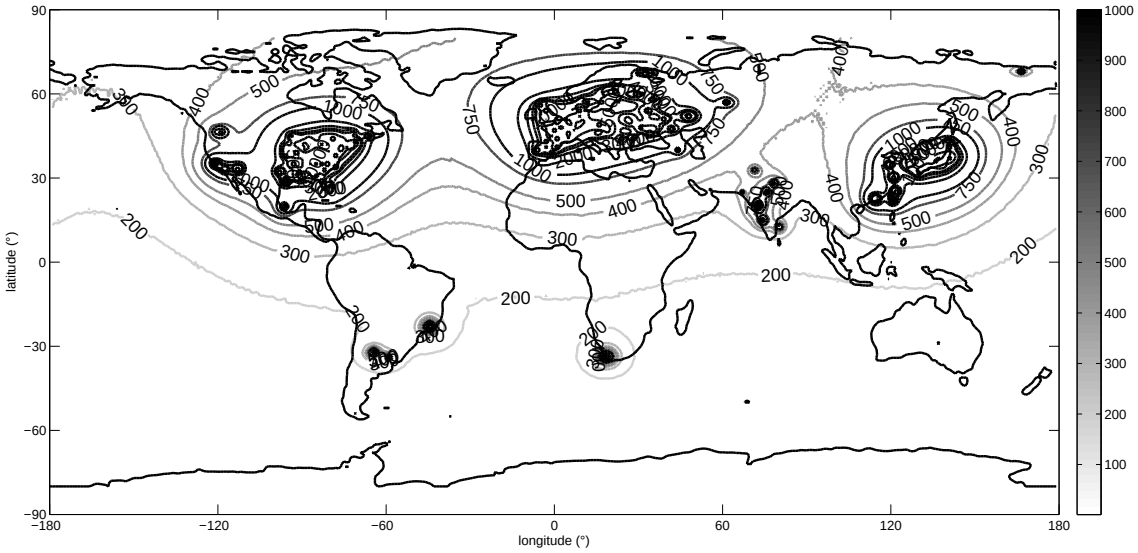

FIG. 2. Maps illustrating the number of neutrino events that would be detected in a 10^{34} free protons detector ($E_{vis} > 2.6$ MeV, 4 kmwe operating depth) after half a year of data taking. 192 nuclear power stations have been included, accounting for a 78% global load factor. This map includes all non neutrino backgrounds which are negligible at this depth in the northern hemisphere (see Section VI).

commercial nuclear reactors is far greater than that of research reactors. In this work we consider only power reactors with thermal power greater than 100 MW_{th}, and we do not account for research reactors. This assumption is correct for most locations around the worlds, but it may be locally inexact in some areas with no power stations.

To be able to detect a clandestine reactor and locate undeclared nuclear fission activities we must know the event rate coming from regular power reactors, at any place and time. We assume a 3% uncertainty [36]. Obviously it would be harder to detect clandestine activity in areas where commercial and/or research reactors activity is high. We computed the number of expected antineutrinos accounting for a detection efficiency of 80%, in our baseline 138,000 ton detector. The number of events detected as a function of geographical position on Earth is shown in figure 2, for half a year of exposition corresponding typically to the time needed to search for a rogue activity. This computation accounts for the state-of-the-art flavor neutrino oscillations. The mean load factor of each reactor for the 1998-2008 period has been included when possible.

B. Geoneutrinos

Geoneutrinos are natural anti-electron neutrinos arising from the decay of radioactive isotopes of uranium, thorium, and potassium in the crust and mantle of the Earth. The spectrum of neutrinos from the decay chains of uranium and thorium extends above the energy threshold for inverse neutron decay (1.8 MeV) to the maximum geologic antineutrino energy (3.27 MeV), corresponding to a 2.5 MeV visible energy deposition in a liquid scintillator detector. Potassium neutrinos are below threshold for this reaction. For the current study we used a 2° x 2° map providing the Uranium and Thorium geoneutrino fluxes based on the Earth reference Model in [39]. Geoneutrino fluxes are computed following the prescription described in [40], at the detector longitude and latitude coordinates, including neutrino oscillations. The geoneutrino background rate ranges from a few hundred interactions per 10^{34} H.year in the middle of the oceans (thin oceanic crust), to a few thousand interactions per 10^{34} H.year in the middle of the continents (thick continental crust). A possibility to discard this background completely is to set an analysis threshold above 2.5 MeV. Another possible source of background is the georeactor which is a hypothetical natural nuclear reactor in the core of the Earth [41] . In our study we neglect its potential influence.

V. TOWARDS AN UNDECLARED REACTOR SIGNAL

Our purpose is to provide a method to detect clandestine nuclear activity within a few months of observation. An undeclared reactor operating at a given power would stand out in the received $\bar{\nu}_e$ rate. As a baseline we consider several a 10^{34} free protons liquid scintillator detector, fitting inside an oil supertanker. The strategy is to deploy one or more of these detectors as close as possible to a suspicious area, typically between 100 and 400 km. The detectors are then temporarily sank underwater for data taking until a significant amounts of events are detected. In this section we detail the statistical method used to decide whether a signal of undeclared activity is seen above the background, at a given confidence level.

A. Defining a decision threshold

Let b be the background, i.e. the average number of events occurring in the detector in the absence of any clandestine activity. Either from past measurements, or theoretical calculations or other input, b is known with a certain uncertainty σ_b. We will treat this error as Gaussian. Now let n be the number of events actually observed in the detector. The first question one can ask is whether n is compatible with a fluctuation of the background, or whether it is too high and could therefore be a sign of suspicious activity. This is a well known problem, studied in great details in e.g. [42]. We will simply reproduce some of the explanations and calculations therein. Following Currie's notation, we will write L_C the *decision threshold* or *critical level*: it is the observed number of events above which the operator will declare having observed a positive signal, i.e. detected a possible clandestine reactor. Of course this level depends on the rate of false alarms (incorrect reported detection while no clandestine reactor is present, also known as type I error) that one is willing to tolerate a priori.

In the absence of any clandestine reactor, n follows a Gaussian distribution, with mean b and error $\sqrt{b+\sigma_b^2}$. Given a certain confidence level α,

$$n < b + k_\alpha \sqrt{b+\sigma_b^2},$$

where k_α is the α quantile of the normal distribution. Consequently,

$$L_C = k_\alpha \sqrt{b+\sigma_b^2}.$$

If, having observed n events, $n - b > L_C$, then the detector will report the presence of a clandestine reactor, with a pre-determined false alarm rate $1-\alpha$.

This criterion has the advantage of being directly applicable to data, and is used to make a decision on whether to take further action. It depends solely on the mean and uncertainty on the background, and the chosen confidence level. Note that at this stage there is no localization of the detector. The purpose of L_C is to decide whether the observation signals suspicious activity or not.

B. Defining a detection limit

Following [42], we can also determine L_D, the *minimum detectable signal*, viz. the minimal amount of signal that could a priori be detected. For this purpose it is first necessary to determine L_C at a certain false alarm rate α, as explained in the previous section. We then define a second confidence level β, controlling the amount of type II error that we tolerate: β is the probability that an existing reactor would be missed by our method. With these definitions, L_D is the average amount of signal that would lead to detection (i.e. observation of more than L_C counts) with probability $1-\beta$. The solution to this problem is found in [42]:

$$L_D = L_C + \frac{k_\beta^2}{2}\left(1 + \sqrt{1 + \frac{4L_C}{k_\beta^2} + 4\frac{L_C}{k_\alpha^2 k_\beta^2}}\right). \quad (1)$$

With these two quantities, we can explore the sensitivity and power of our detection method.

C. Expected sensitivity including reactor neutrino background only

In this section we will study L_C and L_D, as a function of the detector mass, exposure time, clandestine reactor thermal power, and the commercial neutrino background rate at any Earth location.

Let us introduce a new luminosity unit, called the r.n.u. (for reactor neutrino unit) and defined as 1 r.n.u. = 0.197 10^{30} MeV. With this unit, an experiment taking data for T years with a total clandestine nuclear power of P GW_{th}. and with N 10^{34} free protons inside the target has a luminosity $\mathcal{L} = T\,P\,N$ r.n.u.. The expected number of events, $N(L)$, at a distance L from a reactor, assuming no - oscillation, is

$$N(L) = \frac{\langle\sigma_f\rangle}{4\pi\,\langle E_f\rangle}\frac{\mathcal{L}}{L^2} \simeq 230\,\left(\frac{T}{0.5\text{ y}}\right)\left(\frac{P}{100\text{ MW}}\right)\left(\frac{N}{10^{34}}\right) \quad (2)$$

The rate in equation 2 is then corrected for neutrino oscillations in all our calculations. Figure 3 provides the maximum power of an undeclared nuclear reactor consistent with the neutrino background as a function of the reactor distance and neutrino background from commercial nuclear power stations, setting a 10% false alarm tolerance (type I error). One can identify three representative situations of the commercial reactor background level: a low

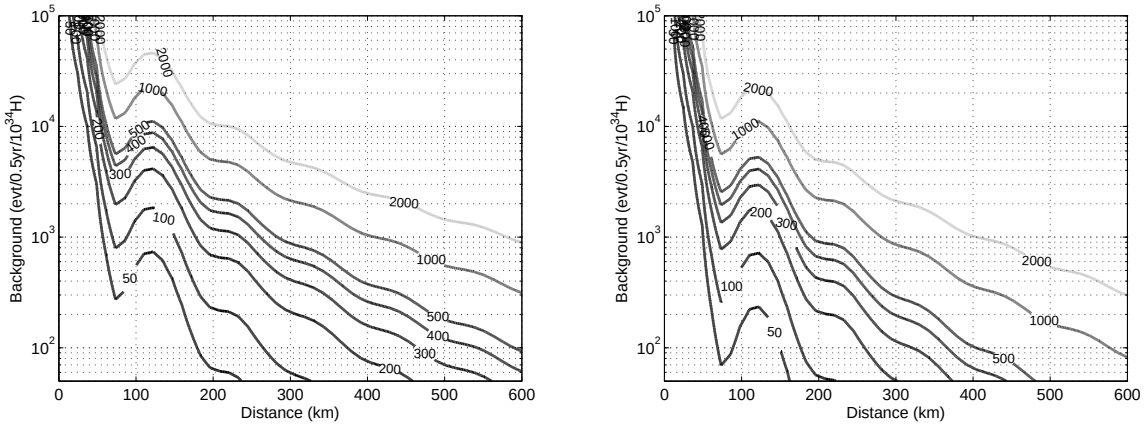

FIG. 3. (left) Maximum power (in MW) of an undeclared nuclear reactor consistent with the neutrino background as a function of the reactor distance (km) and neutrino background from commercial nuclear power stations, as described in section V A. We set a 10% false alarm tolerance. (right) Minimum power (in MW) of an undeclared nuclear reactors that could a priori be detectable by the neutrino method as a function of the neutrino background and the reactor distance (km), as described in section V B. The false alarm rate is 10% and the probability of missing an existing reactor is 10%. In both cases the detector has 10^{34} free protons and operates for 6 months, with $E_{vis} > 2.6$ MeV. Wiggles between of 50-150 km are induced byΔm^2_{21} driven neutrino oscillations supressing the electron antineutrino signal.

background area, corresponding to the southern hemisphere, where the detector would detect 10^2 background events in 6 months; a medium background area corresponding to 10^3 events; an a high background area corresponding to 10^4 events, near clusters of nuclear power stations. Figure 3 provides also the minimum power of an nuclear reactor detectable by the neutrino method as a function of the neutrino background and the reactor distance. The false alarm rate, or type I error, is 10% and the probability of missing an existing reactor, or type II error, is 10%. In medium background conditions we note that a 300 MW reactor could be detected in 6 months with single a 138 kt liquid scintillator detector located 300 km away.

VI. DETECTOR BACKGROUNDS

Irreducible commercial reactor neutrinos are not the only source of backgrounds. Non-neutrino backgounds could prevent any neutrino detection if not handled properly. Indeed the expected low signal event rate must not be drowbed by a high rate of background events. This implies extensive passive shielding to protect the fiducial volume from natural radioactivity, as well as active shielding to veto cosmic rays. In addition, hundreds to thousands of meters of water are mandatory to achieve sufficiently low levels of atmospheric muons, neutrons and cosmogenic radioisotopes. In this section we review the available detection technologies. We then provide a modelization for the three main kinds of non antineutrino background: accidental coincidences, fast neutrons and the long-lived muon induced isotopes ^{9}Li/^{8}He, as a function of the operating depth.

A. Liquid scintillator and Water Cerenkov technologies

Liquid scintillators have commonly been used for the past 60 years to detect neutrinos using the inverse β-decay reaction. The hydrogen atoms serve as targets to neutrinos, producing ionizing particles. The liquid scintillator emit light in the UV-range when crossed by these charged particles. These liquids can be flammable or dangerous to the environment and thus require special care when large amounts are handled, as discussed in the article. The inverse beta-decay reaction does not allow to recover the direction of the incoming neutrino, apart from a slight backward shift of the positron production. The scintillation light, isotropically emitted, allows to find the position of the neutrino interaction within a few tens of centimeters. Large volume detectors may yield a few hundred of photoelectrons per MeV deposited, corresponding to an energy resolution of a few percent even for the less energetic neutrino detected. This detection technology based on liquid scintillator has the capability to measure the full $\bar{\nu}_e$ spectrum since the instrumental threshold may be lowered to 1 MeV or less, depending on backgrounds.

High purity water is also used as a detection medium for charged particles traveling through at super-luminous speed [16], inducing so-called Cerenkov radiation. Water has a few advantages: it is straightforward to handle, non flammable, non toxic, available in large volumes at relatively low cost, and easily purified by common techniques

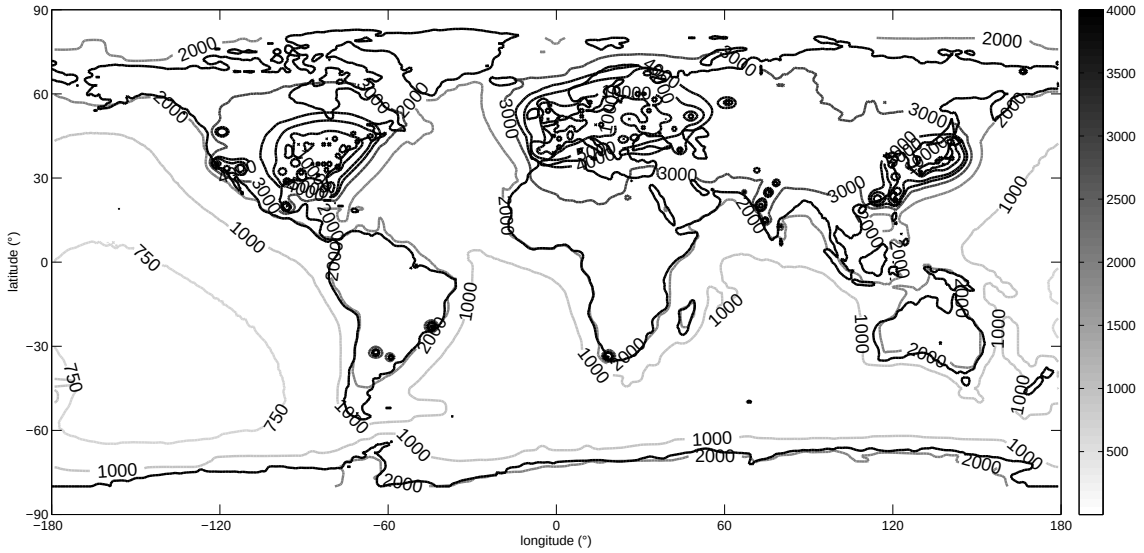

FIG. 4. Maps illustrating the neutrino and non-neutrino background events that would be detected in a 10^{34} free protons detector (1 MeV energy threshold), operating for half a year at a depth of 2,5 kmwe. A distances greater than 1,000 kilometers from nuclear power station clusters, the rate is dominated by geoneutrino events (see Section IV B). This background could be rejected by setting an analysis threshold $E_{vis} > 2.6$ MeV.

to improve its transparency. For charged particles above an energy threshold (0,78 MeV for electrons) only 200 UV photons/cm are emitted along the track, ie roughly 30 times less light than liquid scintillators. Similarly this detection technique cannot be used to determine the direction of the incoming neutrino.

For both technologies, doping the liquid with Gadolinium at the level of 1–5 g/l can greatly improve the sensitivity to electron anti-neutrinos from reactors. The large cross section for neutron capture on ^{157}Gd ($2.59 \cdot 10^5$ barn) and ^{155}Gd ($6.1 \cdot 10^4$ barn) enhances the sensitivity to the delayed neutron signal. The positron, emitting scintillation photons or radiating Cerenkov photons, is immediately detected with or without gadolinium. However the neutron, quickly thermalized in the hydrogen riched mediums, is captured on Gd with a probability of more than 80%. Upon capturing a neutron, a Gadolinium nucleus relaxes to its ground state by emitting a cascade of gamma rays having a total energy of about 8 MeV, thus enhancing the detection efficiency. This is especially true in water where the neutron capture signal on hydrogen, at 2.2 MeV, is barely detectable above backgrounds. Furthermore the time delay between the positron and neutron events is significantly decreased leading to a reduction of accidental backgrounds. Unlike Gadolinium-doped water, stable Gadolinium-doped liquid scintillators are difficult to obtain, but we assume that current technologies being developed for the next generation of experiment [15] will be routinely available thirty years from now.

B. Accidental backgrounds

When detecting antineutrinos, naturally occurring radioactivity (U, Th, K) of the component of the detector may create fake signal - so-called accidental background - defined as a coincidence of a prompt energy deposition between 1 and 10 MeV, followed by a delayed neutron-like event, occurring after a delay τ_d of a few hundredths of a millisecond, in close proximity to the prompt energy deposit (within a volume $V_d \sim 1m^3$). With these notations, the accidental background rate r_{acc} is given by $r_{acc} \sim r_p\ r_d\ \tau_d\ V_d\ V_{det}$, where r_p and r_d are the specific background rates (in units of $\mathrm{sec}^{-1}\mathrm{m}^{-3}$) for the prompt and the delayed signal, respectively. V_{det} is the total detection volume.

The potentially most dangerous of these backgrounds are those caused by radioactive impurities within the active detection liquid. The use of standard techniques like distillation, water extraction, nitrogen purging, and column chromatography allows to achieve sufficiently low concentrations in radio–impurities [28, 29]. The detection liquid is contained in a vessel and photomultipliers

Experiment	**KamLAND**	**Borexino**	**SNIF extrapolated from**	
Label			KamLAND	Borexino
Flat eq. depth	2.05 kmwe	3.05 kmwe	2.5 kmwe	
Scintillator	$C_{11.4}H_{21.6}$	C_9H_{12}	$C_{16}H_{30}$	
H/m^3	6.60 10^{28}	5.30 10^{28}	6.24 10^{28}	
C/m^3	3.35 10^{28}	3.97 10^{28}	3.79 10^{28}	
density	0.78	0.88	0.86	
Mass (tons)	912	278	138 000	
Volume (m^3)	1170	316	160 000	
Radius (m)	6.5	4.25	23	
Cyl. Length (m)	—	—	96.5	
$\mu-$Section (cm^2)	1.3 10^6	0.57 10^6	44 10^6	
$\mu-$Flux (cm^{-2}s^{-1})	1.6 10^{-7}	0.3 10^{-7}	0.7 10^{-7}	
$\mu-$Energy (MeV)	219	276	247	
$\mu-$Rate (s^{-1})	21.3 10^{-2}	1.6 10^{-2}	9.5	
$\mu-$DT (200μs)	4 10^{-5}	0.3 10^{-5}	60 10^{-5}	
Co-DT (200 ms)	4 10^{-2}	0.3 10^{-2}	60 10^{-2}	
Exposure (H.year)	2.44 10^{32}	6.02 10^{30}	10^{34}	
Threshold (MeV)	0.9	1	0.9	1
Accidental Rate	80.5±0.1	0.08±0.001	3300±4	133±2
Li/He Rate	7.0±1	0.03±0.02	85.9±12.2	108±71.9
Fast n Rate	9±9	0.025±0.025	171±17	93.4±9
Geo-ν	69.7	2.5±0.2	2860	4150±332
Reactor-ν	1609±51	5.7±0.3	65900±2080	9460±498

TABLE I. Breakdown of the background estimates for SNIF. We consider two different background measurements from the KamLAND and Borexino antineutrino searches [30, 36]; Cosmogenics from KamLAND are rescaled from [31]. $\mu-$DT and Co-DT are the estimates of both muon- and cosmogenics-induced dead time (DT). The flat equivalent depth are taken from [34]. Extrapolation to SNIF corresponds to a 10^{34} proton detector operating for 1 year at a depth of 2.5 kmwe, according to the prescription given in [33, 34]. In this table, SNIF is taken to be located at the KamLAND/Borexino sites to calculate Geo- and Reactor-neutrino backgrounds. Geo-neutrino rates are measured, in agreement with the reference Earth model [43].

catch the light emitted in the antineutrino interaction. Those materials and equipments also contain radioactive impurities whose decay products may release their energy within the liquids. The selection of high purity materials entering the detector (mechanical structures, photomultiplier tubes) as well as passive shielding provide an efficient tool against this type of background. Surface/wall-induced events could be rejected through spatial reconstruction cuts, with a loss of target mass however. Taking accidental backgrounds into account leads to the detector design presented in Section VIII.

In Table I we present our background rescaling results. We use r_p and r_d values measured in Borexino and KamLAND, thus the accidental background rate in SNIF scales with V_{det} only. We rescale the estimated rates for a 10^{34} proton.year target immersed in deep water (SNIF baseline design). By choosing the Borexino extrapolation providing the lowest estimate we note the accidental background dominates the cosmogenics backgrounds at depth below 2 kmwe, as displayed in Figure 5 . This is justified assuming a detector as radiopure as Borexino could be achievable at the SNIF scale within the next 30 years. Considering no scaling of the delayed signal background may be too simplistic, however. In order to get a more robust result in our current study we get rid of the accidental background contribution by setting an analysis threshold $E_{vis} > 2.6$ MeV. This implies a loss of signal statistics of 28 %, but it also relaxes the radiopurity constraints by orders of magnitude, simplifying the project feasibility.

C. Operating depth constraint based on cosmic muons rate

The cosmic-ray muon flux underwater can be deduced from data at different depths and extrapolated as a function of equivalent water depth where 105 g/cm^2 = 1000 m.w.e. Using the depth–intensity relation for the total muon flux with a flat overburden given in [34] we derive the muon rate in a detector containing 10^{34} free protons having a section exposed to muons of 1.48 10^8 cm^2 (cylinder of r=23 m radius and l=96.5 m length). At water depths of 500 m, 1000 m, 2000 m, and 4000 m we obtain a muon rate of 560, 110, 8, 0.3 Hz, respectively. Vetoing the detector for 200 μsec after each muon would thus lead to respective muon- induced dead times of 11%, 2,2%, 0,15%, and 0,006%. From this data we derive the minimum operating depth of a 10^{34} protons module at around 0,5 km, not accounting for backgrounds yet. We include this depth-dependent dead time in our sensitivity estimates. In order to reduce the dead time at shallower depth the detector should be subdivided internally in optically decoupled compartments as described in Section VIII.

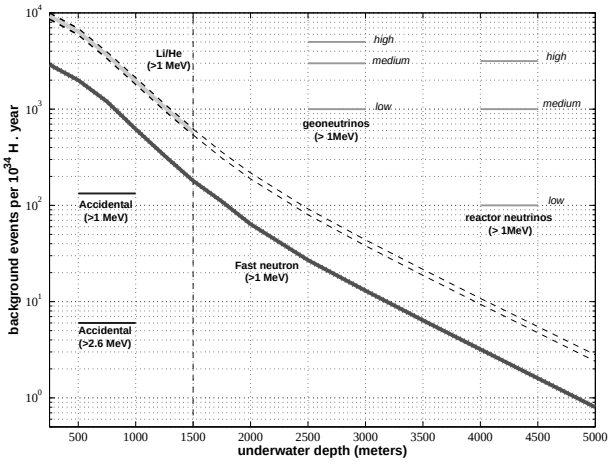

FIG. 5. Evolution of the cosmogenics and fast neutrons background with respect to the depth of the detector in kmwe for a detector module containing 10^{34} free protons taking data for a year. Fast neutron and cosmogenic backgrounds are estimated with the models presented in sections VI D 2 and VI D 1. It is worth noting that cosmogenics could be neglected at a depth greater than 1500 mwe, with an additonal 10% dead time. For comparison we indicate our estimates of accidental backgrounds for two different thresholds, 1 and 2.6 MeV (visible energy). We also give three possible estimates for the geoneutrino rates, for continental crust areas (high), coast areas (medium), and oceanic crust areas (low) [38]. Commercial reactor neutrino background under three hypothesis are also displayed for comparison (see section IV).

D. Correlated backgrounds

Cosmic ray muons will be the dominating trigger rate at the depth of our detectors. Their very high energy deposition corresponds to about 2 MeV per centimeter path length and provides thus a strong discrimination tool. They induce the main source of of dangerous events, cosmogenic activity and fast neutrons, mimicking the antineutrino signal.

1. Muon induced cosmogenic activity

Energetic muons can interact with carbon nuclei producing by spallation radioactive isotopes such as ^{8}He, ^{9}Li and ^{11}Li. These nuclei are unstable and decay emitting an electron and a neutron, thus mimicking perfectly the signal from an antineutrino interaction ; moreover the long lifetime of these nuclei, a few 100 ms, complicate the task to identify them. This background is considered as the most serious difficulty to overcome for our project, driving the operating depth of the detector. When this background is reduced - roughly below 3500 mwe - ^{8}He, ^{9}Li and ^{11}Li decays could be identified through a four-fold coincidence ($\mu \to n \to \beta \to n$) characteristic signature.

In order to estimate the cosmogenic backgrounds we used the rates experimentally measured by the Kamland [31] and Borexino [36] collaborations. The main detector features as well as muon induced backgrounds are provided in Table I. The production rate of cosmogenic radioisotopes is proportional to the muon flux (Φ_μ), the cross section $\sigma_{tot}(E_\mu) \sim E_\mu^{0.73}$ [33], and the total number of carbon nuclei. We start from the muon flux predictions at the flat equivalent overburden of the KamLAND (2.05 kmwe) and Borexino (3.05 kmwe) locations. We then rescale the backgrounds to 10^{34} proton.year for different depths according to the total muon flux, and energy formulae given in [34]. Estimates are corrected according to the different carbon composition in Borexino, KamLAND and SNIF liquid scintillators. Results for a 10^{34} proton.year target deployed at a depth of 2.5 kmwe are presented in Table I. An additonal selection of events with $E_{vis} > 2.6$ MeV would reject 23% of the cosmogenic background, according to the simple spectrum shape presented in [35]. In this work we envisage a further possibility of erradicating the cosmogenics backgrounds by vetoing the detector after each muon for a long enough time. We veto a 3-m-radius cylinder around each muon track for 600 ms (3 times the ^{8}He, ^{9}Li decay time periods). Neglecting the veto inefficiency we find that this technique could only be effective at operating depth greater than 1,5 kmwe to preserve a dead time below 10% in a 138 kton detector. We thus neglect the cosmogenics backgrounds from this depth on. Below 1,5 kmwe we considered the KamLAND rescaling from [31]. The evolution of the predicted cosmogenics background in SNIF with respect to the detector depth is presented in Figure 5.

For completeness we note that a water Cerenkov detector is less affected by this specific background [32] thanks to the lower yield of these nuclei when spallation reaction are on oxygen nuclei.

2. Muon induced fast neutron activity

An important source of background comes from neutrons produced in the surrounding of the detector by cosmic ray muon induced hadronic cascades. The difficulty is that the primary cosmic ray muon may not penetrate the detector, being thus invisible. This is especially true for a small detector. These processes produce arbitrarily high energy neutrons inducing proton recoils mimicking the prompt signal, and then producing the coincident neutron signal after thermalization and capture. Such a sequence can mimic a $\bar{\nu}_e$ event. At several hundred mwe, muon-induced neutron production can be fairly well estimated from the results of previous underground experiments, like KamLAND [30] and Borexino [36]. Fast neutrons can indeed be produced by muons either crossing the inner stainless steel vessel or interacting in the

water around the detector. We estimate the rate of fast neutrons by scaling the KamLAND and Borexino results according to the procedure described in Section VI D 1. Results for a 10^{34} proton.year target deployed at a depth of 2.5 kmwe are presented in Table I. An additonal selection of events with $E_{vis} > 2.6$ MeV would reject 31% of the fast neutrons background, assuming an energy-flat spectrum.

For SNIF we only consider the case of Borexino and we reduce the neutron production from the rock (4/5 of the total rate) by a factor of 2.7 in order to correct for the lower density of the water. Contrary to smaller detectors like KamLAND and Borexino, in very large detectors like SNIF the fast neutron background could be considered as a surface background. We thus assume that the fast neutrons induced by muons crossing the bulk of the detector could be perfectly tagged in a very large liquid scintillator detector (neglecting tiny veto inefficiencies). The dominant fast neutron component induced by the water surrounding the detector can only be detected at distances less than 3 meters from the detector inner vessel walls. Further inside the detector fast neutrons will have been significantly slowed. This lowers the estimated background by 70%. The evolution of our predicted fast neutron rate with respect to the detector depth is depicted in Figure 5. We assume an uncertainty of 10%, achievable within the next 30 years.

E. Impact of the backgrounds on the rogue reactor sensitivity

In this section we discuss for the first time the impact of the non-neutrino backgrounds on the sensitivity of the neutrino method to detect undeclared nuclear fission activities. Our baseline exposure is a 10^{34} free protons detector operating for 6 months. Figure 2 provides the antineutrino rate world map at an operating depth of 4 kmwe. Correlated background, included as described in Section VI, turns out to be negligible at this depth. We apply a 2.6 MeV visible energy threshold, rejecting accidental and geoneutrino backgrounds. We clearly see the high antineutrino rate from nuclear commercial power stations around Europe, US, and Japan. With an expected rate of a few thousand events one can barely detect a 500 (300) MW reactor from a distance of 300 (200) km. Detailed results are displayed in Figure 3. South of the equator the contibution of antineutrinos from commercial power stations in reduced to 400 or less hundred events, allowing the detection of a 300 MW reactor from a distance of 300 km .

The antineutrino world map rate of figure 4 illustrates the backgrounds that would occur, with a 1 MeV visible energy threshold, at a depth of 2,5 kmwe. At distances of more than a thousand kilometers from nuclear power station clusters the rate is dominated by geoneutrino events. This justifies the choice of setting a 2.6 MeV visible energy threshold to be able to detect a reactor of less than 1 GW in the regions of interest.

The influence of backgrounds on the sensitivity to rogue activity is illustrated in figure 6, as a function of the operating depth and of the expected antineutrino background from nuclear power stations. In this case we assume the existence of a 300 MW rogue reactor. We first notice that for a neutrino background of more than a thousand events the sensitivity is not affected by the operating depth because the non-neutrino background is negligible (assuming more than 500 mwe). In accordance with Figure 3 we find a maximum detection distance of 300 km if the depth is greater than 1,5 kmwe. At 0,6 kmwe the detection distance would be degraded to 200 km. The right panel of Figure 6 clearly shows the correlation between the minimum operating depth in order to be free of non-neutrino backgrounds versus the commercial reactor neutrino backgrounds. With our baseline exposure of $0.5\,10^{34}$ H.y we conclude it is not necessary to deploy a detector module below 2 kmwe.

In order to understand the limitation of the neutrino method we now consider an exposure of $0.5\,10^{35}$ H.y. This could be realized with five detector modules of 138 kt operating for 1 year. Results are displayed on Figure 7. For a typical southern hemisphere background of 3000 events we see that we become sensitive to a 50 MW reactor from a distance of 200 km. The right panel of the figure shows how the sensitivity evolves with the operating depth, still allowing the detection of a 75 MW reactor at a distance of 150 km with a detector operating under 750 mwe.

VII. CLANDESTINE REACTOR LOCALIZATION

The strategy developed in this article is to deploy a detector as close as possible to a suspicious area to find evidence of a clandestine activity. We arbitrarily make the choice of setting the false alarm threshold to 10% and the detection confidence level at 90%. If any evidence of clandestine activity is found, additional detectors have to be deployed with the objective of finding the clandestine reactor's location. Four detector modules (i=1,2,3,4) operating at four distinct locations $(\lambda,\phi)_{di}$ with a positive decision threshold are necessary to determine a unique location, inferring in addition the reactor's thermal power. We present here an optimization algorithm providing an approximate position of the presumed clandestine reactor as well as confidence levels of the clandestine reactor location, for the best fitted thermal power. For simplicity we assume the reactor to be constantly running.

Let's assume the presence of a undeclared reactor with a power P (MW) at a given location $(\lambda,\phi)_R$. S_i is the neutrino signal induced by the rogue reactor in the detector i. The signal is drawn according to a poissonian distribution of mean S_i. B_i is the expected background, including known nuclear power stations and non-neutrino backgrounds. All background errors described in Sec-

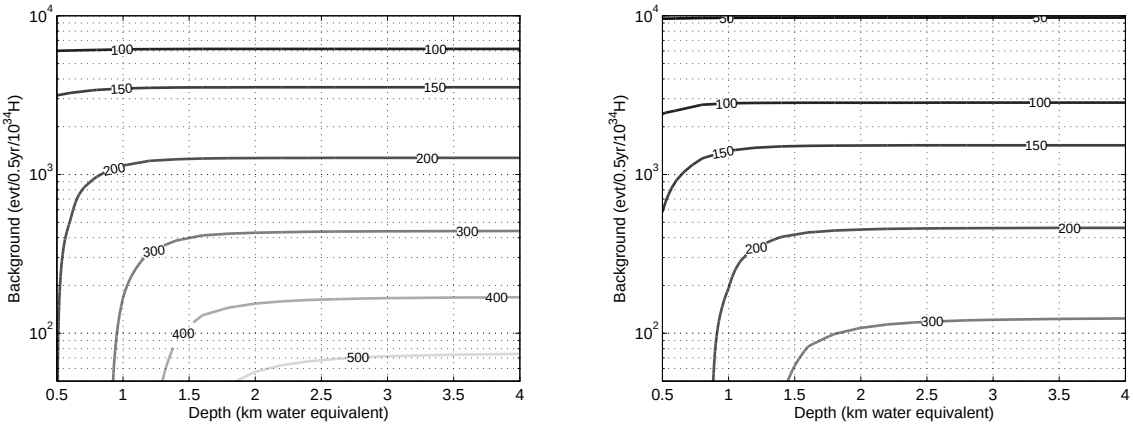

FIG. 6. These graphs describe the effect of the non-neutrino backgrounds as a function of the operating depth, assuming a 300 MW undeclared reactor, investigated by a 10^{34} free protons detector operating for 6 months with a detection threshold $E_{vis} > 2.6$ MeV. In this study we included all known sources of backgrounds (geoneutrinos, reactor antineutrinos, accidental, cosmogenics, and fast neutrons) as described in VI. The left panel describes the minimum distance (km) at which the signal from the clandestine reactor is consistent with the background expectation, as a function of the detector depth and reactor neutrino backgrounds, with a 10 percent false alarm tolerance (see section section V A). The right panel shows the maximum distance (km) at which one could a priori detect a rogue activity of 300 MW with 90% probability (see section section V B).

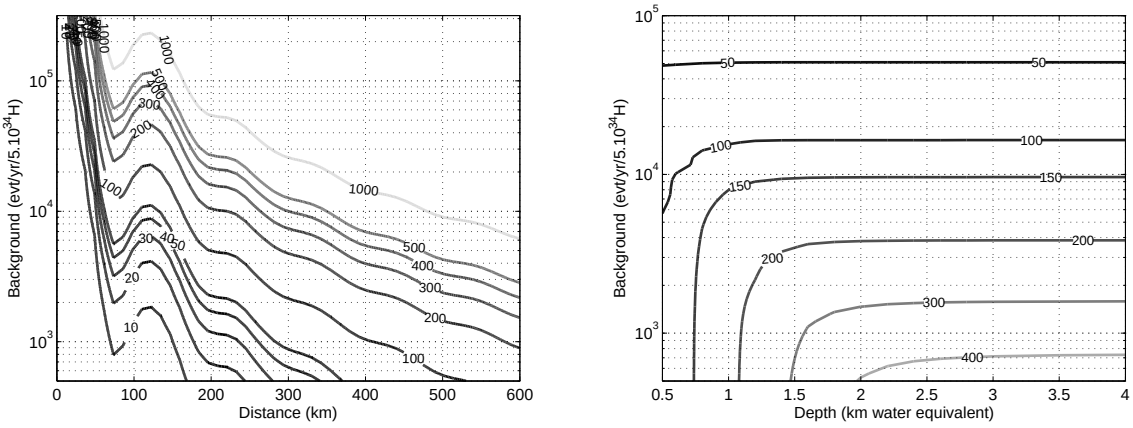

FIG. 7. These graphs describe the effect of the non-neutrino backgrounds as a function of the operating depth, assuming a 75 MW undeclared reactor searched for by five 10^{34} free protons detector modules operating for one year with a detection threshold $E_{vis} > 2.6$ MeV. We included all known backgrounds as described in VI. The left panel shows the maximum power (in MW) of an undeclared nuclear reactor consistent with the neutrino background as a function of the reactor distance (km) and neutrino background from commercial nuclear power stations, as described in section V A. We set a 10% false alarm tolerance. The right panel describes the minimum distance (km) at which a 300 MW rogue reactor is consistent with the background expectation as a function of the detector depth and reactor neutrino backgrounds, with a 10 percent false alarm tolerance (see section section V A). Note that the reactor neutrino background is rescaled by a factor 10 with respect to Figures2 and 4.

tions IV and VI are added in quadrature. O_i is the observed value in the detector i, following a gaussian of variance O_i (statistical error). The triplet $(\lambda,\phi,P)_R$ is estimated by minimizing the χ^2 function :

$$\chi^2 = \sum_i \frac{(O_i - S_i(\lambda,\phi,P)_R - B_i)^2}{B_i + S_i(\lambda,\phi,P)_R} \qquad (3)$$

With four detectors the $\Delta\chi^2$ function follows a χ^2 distribution with $4-3=1$ degree of freedom, allowing to derive the $(\lambda,\phi)_{CL}$ confidence intervals at the CL=68,3% (1σ) and CL=95,4% (2σ) by selecting respectively the $\Delta\chi^2 = \chi^2(\lambda,\phi) - \chi^2_{min}$=2,30 and 6,18 areas. Note that the thermal power is fitted at each point on the contour map. Any external information providing the thermal power would thus greatly enhance the localization algorithm, with a possible reduction of the number of detec-

tors to three.

The accuracy and robustness of the method depends strongly on the location of the rogue activity. Let's illustrate the localization in three distinct geographical configurations, a reactor located on a penisula, a reactor located on an island, and a reactor located on a flat shore. In all cases we have selected a region with a commercial neutrino background of several hundreds of counts per 10^{34} H.y corresponding to equatorial regions for instance.

A. Peninsula

The first case, presented on Figure 8, assumes a 300 MW_{th} clandestine reactor located in a peninsula surrounded by water. We placed the reactor at the origin of our coordinate system. Four detectors are deployed at 1 kmwe, between 209 and 264 km from the clandestine reactor. They operate for 1.0 year. Though the true latitude and longitude coordinates of this exemple are hidden in the figure, all world commercial reactor neutrino backgrounds are included, providing 631 events on average, to be compared with a mean rogue signal of 75 events. The clandestine reactor is clearly detected (see Table II). Its position is reconstructed within the 90% confidence interval, but with a largely overestimated power of 737 MW. In order to assess the resolution of

(λ,ϕ)	**Distance**	<**S**>	<**B**>	**O**	L_c	**O**-L_c
(**-1.0°**,**+1.6°**)	209 km	101	643	774	54	131
(**+0.1°**,**+2.1°**)	234 km	86	645	753	54	108
(**+2.6°**,**+0.2°**)	286 km	52	628	635	53	7
(**+1.3°**,**-2.0°**)	264 km	63	610	713	53	103

TABLE II. Four detectors containing 10^{34} free protons are located at an average distance of 250 km from an undeclared reactor located in a peninsula. Each detector module of 138,000 is operating in the sea at a depth of 1 kmwe, for 1 year. S is the signal coming from the rogue reactor. B is the expected background, including neutrinos from known nuclear power plants and non-neutrino backgrounds. O is the observed value according to an experimental trial. L_c is the decision threshold value. **O**-L_c is the 'distance' of the observation with respect to the decision threshold.

the neutrino method we draw 1000 random trials of the peninsula experiment described above, and then reconstruct the reactor's position and power. After excluding 125 anomalous fits we could reconstruct the reactor position within 133 km in 68% of the case (see Figure 9). The mean reconstructed thermal power is 244 MW with a standard deviation of 101 MW.

B. Island

The second case, presented on Figure 10, assumes a 300 MW_{th} clandestine reactor located in an 500 km x 500 km

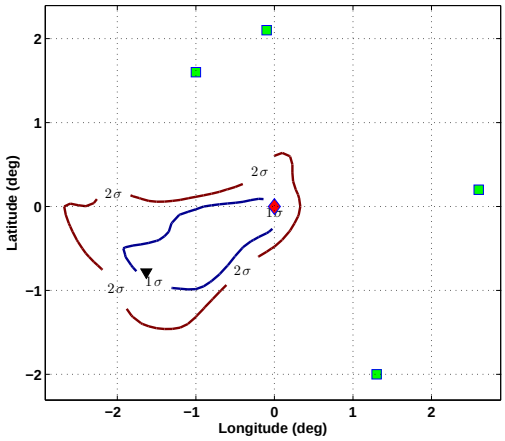

FIG. 8. This figure demonstrates the ability of four 10^{34} protons detectors (squares), to detect and locate a 300 MW_{th} clandestine reactor (diamond) located on a peninsula. The triangle shows the reconstructed position at the best fitted power. The contours provide the 68,3% and 95,4% confidence levels for the clandestine reactor location. The thermal power at best fit is $P = 737$ MW_{th}.

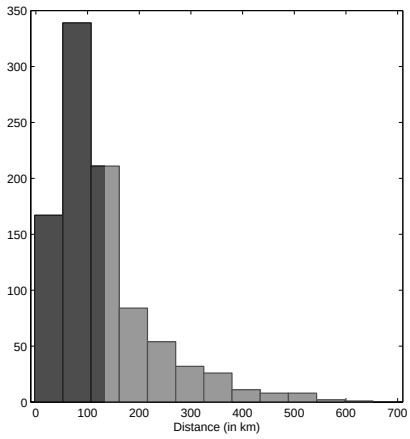

FIG. 9. Distribution of the distance (km) between the true and the reconstructed position for 875 trials of the peninsula experiment. The spatial resolution, estimated as the 68% quantile, is 133 km (dark gray area).

island. We choose the reactor at the origin of our coordinate system. Four detectors are deployed at 1 kmwe, between 156 and 235 km from the clandestine reactor. They operate for 1.5 year. All the known commercial reactors provide 1162 events on average, to be compared with a mean rogue signal of 190 events. The clandestine reactor is unambiguously detected (see Table III). Its position is well reconstructed, within tens of kilometers of the true location, with a slightly underestimated power of 216 MW. This attests to the potential of the neutrino

method. As for the peninsula case we randomely draw

(λ,ϕ)	Distance	<S>	<B>	O	L_c	O-L_c
(+1.5°,+1.5°)	235 km	128	1158	1240	80	81
(0°,-1.4°)	156 km	331	1060	1259	77	199
(-2.0°,0°)	221 km	141	1115	1193	78	79
(-1.0°,+1.5°)	200 km	160	1169	1315	80	145

TABLE III. Four detectors containing 10^{34} free protons are located at an average distance of 203 km from an undeclared reactor located in the middle of a 500 km x 500 km island. Each detector module of 138,000 tons is operating in the sea at a depth of 1 kmwe, for 1.5 year.

1000 trials of the island experiment described above. After excluding 104 anomalous fits we could reconstruct the reactor position within 55 km in 68% of the trials (see Figure 11). The mean reconstructed thermal power is 257 MW with a standard deviation of 67 MW. It

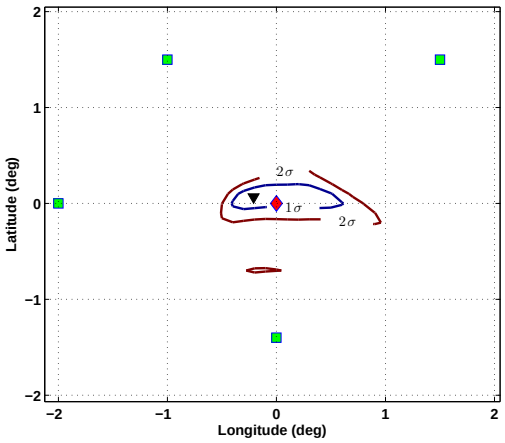

FIG. 10. This figure demonstrates the ability of four 10^{34} protons detectors (squares), to detect and locate a 300 MW_{th} clandestine reactor (diamond) located on an island. The triangle shows the reconstructed position at the best fitted power. The contours provide the 68,3% and 95,4% confidence levels for the clandestine reactor location, for a best-fit thermal power of $P = 216$ MW_{th}. The reactor is clearly located by the neutrino detectors. Superimposition of the true local geographical map allows to exclude the 3σ areas far from the best fit location.

is worth noting that a measurement of the neutrino energy spectrum distorsion due to neutrino oscillation in the undeclared reactor's spectrum observed with a detector located 70–150 km away could improve the precision of the localization. This effect, already measured by the KamLAND detector [30], would however require higher statistics from the undeclared reactor. We will neglect it in our study.

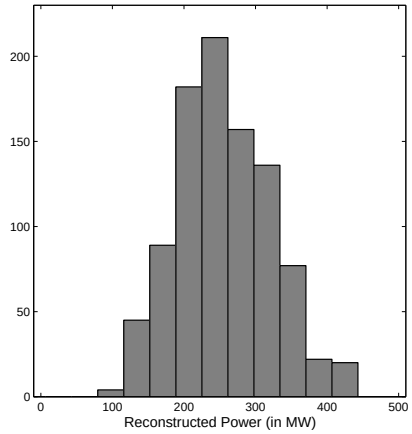

FIG. 11. Distribution of the reconstructed power for 896 trials of the island experiment. The mean reconstructed power is 257 MW with a standard devation of 67 MW.

C. Flat Shore

In the third case, presented on Figure 12, we considered a flat shore along the latitude axis ∼(-0.5° latitude). We articifially placed a 300 MW_{th} clandestine reactor located a few tens of kilometers inland (origin of our coordinate system). Four detectors are deployed at 1 kmwe for 1 year. The relevant information is provided in Table IV). The reactor is clearly localized by each of the neu-

(λ,ϕ)	Distance	<S>	<B>	O	L_c	O-L_c
(-1.2°,+0.6°)	146 km	269	676	943	55	266
(-1.3°,-0.8°)	169 km	168	661	769	54	107
(-0.9°,-1.6°)	200 km	107	655	732	54	77
(-0.9°,+1.5°)	191 km	117	1687	768	55	81

TABLE IV. Four detectors containing 10^{34} free protons are located at an average distance of 177 km from an undeclared reactor located close to a flat shore. Each detector module of 138,000 tons is operating in the sea at a depth of 1 kmwe, for 1.0 year.

trino detectors. On Figure 12 we see 4 possible solutions for the reactor location, the best fit position being reconstructed a few kilometers from the true reactor location. Because of this geometry with the detectors aligned along the shore, we clearly see a degeneracy with the second main solution being reconstructed to the west of the detectors. In this particular case the superimposition of the true local geographical map allows to exclude the three wrong solutions. The flat shore geometry is the most difficult configuration that could lead to broad possible areas for the rogue activity. In such a case, the deployement of an additional detector(s), or the displacement of one of the detectors in the fleet would be necessary to lift the degeneracies.

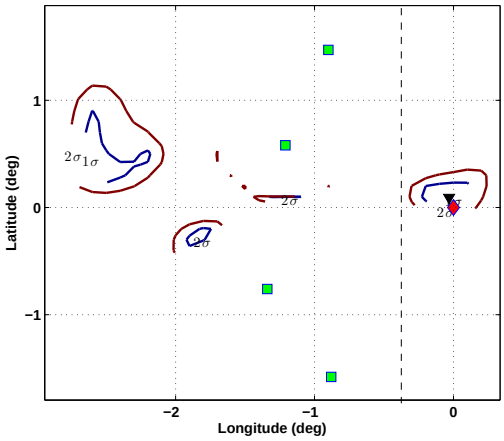

FIG. 12. This figure illustrates the ability of four 10^{34} protons detectors (squares), to detect and locate a 300 MW_{th} clandestine reactor (diamond) located on a flat shore (dotted vertical line), a few tens of kilometers inland. The triangle shows the reconstructed position at the best fitted power. The contours provide the 68,4% and 95,4% confidence levels for the clandestine reactor location, with a thermal power at best fit of $P = 225$ MW_{th}. The solutions west to the detectors are naturally excluded since they are located in the middle of the sea.

VIII. LONG TERM TECHNICAL FEASIBILITY

In this section we address the technical feasibility of the SNIF project within the next 30 years.

We assume that a clandestine reactor neutrino detector would house between 138,000 and 400,000 tons of target liquid in a radiopure environment, designed to be transportable and deployable in the deep ocean. We propose to host the detector in a supertanker to be transported on the detection site. It would then be lowered at a depth of a several hundred meters with a cable deployment system. We will focus our discussion on liquid scintillator technology, being the most efficient electron antineutrino detection medium in large detectors. The design concepts presented here have similarities with those developed for large neutrino detectors proposed for fundamental research, such as Titand [37], Hano-Hano [38] and LENA [44].

The components of the detectors are embedded in each other, the liquid scintillator being in the central volume. The organic solvent under consideration is linearalkylbenzene (LAB, $C_{18}H_{30}$), classically used as an additive to detergents. LAB is currently used in neutrino experiments (for instance SNO+ [25], Double Chooz [26], Daya Bay [27]) because of its good optical transparency (more than 20 m), its high light yield, its low amount of radioactive impurities, and its high flash point (140 degree Celsius) which makes safe handling easier. Moreover experimental studies of temperature and pressure dependence have shown that it is possible to use LAB in a deep underwater environment [38]. Scintillator timing properties as well as optical transparency are improved by adding a combination of solutes, typically PPO (a few g/l) and bisMSB (a few mg/l). In addition, the neutron capture capability of the scintillator is greatly enhanced with the dissolution of a gadolinium complex (1 g/l typically). This should be considered as a serious option if long term stability issues are fully understood. The detection medium would be contained inside a Teflon coated stainless steel tank covered with photomultipliers tubes. In the two extreme cases considered here, the cylindrical tank has the following dimension: r=23 m l=96.5 m to contain 138,000 tons of LAB (160 m^3 for a density of 0.86), and r=25 m l=240 m for the 400,000 ton model (471 m^3), a size approaching the largest supertankers ever built.

Depending on the muon rate, and thus on the operating depth, the central detection volume could be optically segmented by adding disk-shaped stainless steel walls covered with phototubes on both sides. The detector would then contain several optically independent subdetectors, but still allow the liquid scintillator to communicate between the compartments in order to balance the internal hydrostatic pressure. Compensator bags would have to be used inside the tank in order to compensate for volume changes due to compression and temperature variations induced by the underwater deployment. This optical segmentation would improve light collection by reducing the maximum path of optical photons to the photosensors. An optical coverage of the detector walls of 20 percent requires 17,000 photomultipliers of the Superkamiokande type (20 inch) for a 138,000 ton detector, and 41,500 for the 400,000 ton model. We note here that classical phototubes with intrinsic photo-statistical noise of 3 kHz can be used in a gadolinium doped detector without adding backgrounds [47]. Within the next 30 years we can optimistically assume that high-voltage supplies, voltage dividers and signal digitizers could be directly attached to the photomultiplier base [46]. Low power integrated electronics and batteries would have to enable one year of stand alone operation. Neutrino analysis should be done online. Phototube chain implosion has a low probability of occurrence but would lead to the destruction of the detector. Therefore, each individual photomultiplier must be encapsulated in a single acrylics/resin housing. Phototube cells could incorporate an inactive mineral oil or acrylics buffer in front of the photocathode to reduce the accidental background.

In order to further reduce these backgrounds the inner stainless steel tank should be enclosed in another steel vessel providing a protective layer of ultra pure water against external radioactivity. This second detection volume may not be mandatory if the detector were deployed deeper than 2500 meters (10 muons per second only). This external layer could be equipped with photodetectors detecting Cerenkov light from cosmic muons, allowing to further suppress the correlated fast neutron

background. In salt water the dominant single rate background comes from the decay of ^{40}K emitting a 1.4 MeV gamma. As a benchmark, a 1 m-thick water layer would be sufficient to lower the external backgrounds and reduce the fast neutron contribution. For a 138,000 ton detector module this would imply the installation of 4000 additional phototubes on the outer tank wall, and 10,000 for the 400,000 ton version. The number of PMTs could be further reduced by coating the veto with reflective material to enhance light collection, like teflon. In any case the geometry of both tank walls should be curved to accommodate the deep-sea hydrostatic pressure. The detector should finally be zero-buoyant to be sunk into the deep ocean for its operation and to be brought back to the surface for maintenance or redeployment elsewhere. Nitrogen gas could be used to fill up any non liquid part of the detector in order to maintain the scintillator's properties. Setting an analysis threshold $E_{vis} > 2.6$ MeV would greatly reduce the material radiopurity constraints, simplifying the industrialization of the construction.

Thanks to the great progress in antineutrino detection since the 1950s, we believe that a SNIF 138,000 tons detector, containing three times the volume of the largest neutrino detector ever built in the 1990s [16], could be built and deployed in the deep ocean within the next 30 years – not taking into account any financial constraints. The main difficulty will reside in the deep sea deployement.

ACKNOWLEDGMENTS

We would like to thank F. Mantovani for providing us the geoneutrino fluxes map from the Earth model.

[1] http://www.iaea.org/
[2] A. Bernstein *et al.*, J. Appl. Phys. 103, 074905 (2008)
[3] A Porta *et al.*, the Nucifer collaboration, J. Phys.: Conf. Ser. 203 012092 (2010)
[4] J. Learned, Neutrino Conference, Paris (2004)
[5] E. H. Guillian, hep-ph/0607095v2
[6] IAEA Final Report: Focused Workshop on Antineutrino Detection for Safeguards Applications(2008)
[7] P. Vogel and J. F. Beacom, Phys. Rev. D 60, 053003 (1999)
[8] K. Schreckenbach *et al.*, Phys. Lett. B160, 325 (1985)
[9] A.A Hahn *et al.*, 1989, Phys. Lett. B218, 365
[10] Th. Mueller, PhD Thesis, University Paris XI (2010)
[11] Y. Declais *et al.*, Phys. Lett. B338, 383 (1994)
[12] B. Achkar *et al.*, Phys. Lett. B374, 243 (1996)
[13] Apollonio *et al.*, Eur. Phys. J. C27 331-374 (2003)
[14] lbne.fnal.gov/
[15] T. Lasserre and H. W. Sobel, C. R. Physique 6 (2005)
[16] Y. Fukuda *et al.*, Phys. Rev. Lett. 81 (1998) 1562
[17] S. Fukuda *et al.*, Phys. Rev. Lett 86 (2001) 5656; S. Fukuda *et al.*, Phys. Lett. B 539 (2002) 179
[18] Q.R. Ahmad *et al.*, Phys. Rev. Lett. 89 (2002) 011301,011302
[19] S.N. Ahmed *et al.*, nucl-ex/0309004
[20] K. Eguchi *et al.*, Phys. Rev. Lett. 90 (2003) 021802
[21] E. Aliu *et al.*, Phys. Rev. Lett. 94, (2005) 081802
[22] P. Adamson *et al.*, Phys. Rev. Lett. 101 (2008) 131802
[23] http://pdg.lbl.gov/2007/reviews/numixrpp.pdf
[24] earth.google.com/
[25] M. Chen, Nucl. Phys. B (Proc. Suppl.) 154 (2005) 65-6
[26] Double Chooz Collaboration (proposal), hep-ex/0606025
[27] Daya Bay Collaboration (proposal), arXiv:hep-ex/0701029
[28] C. Arpesella *et al.*, Phys. Lett. B 658, 101 (2008)
[29] K. Inoue, hep-ex/0307030
[30] S. Abe *et al.*, Phys. Rev. Lett. 100, 221803 (2008)
[31] S. Abe *et al.*, Phys. Rev. C 81, 025807 (2010)
[32] J. Hosaka *et al.*, SuperKamiokande Collaboration, Phys. Rev. D 73, 112001 (2006)
[33] T. Hagner *et al.*, Astropart. Phys. 14, 33 (2000)
[34] D. M. Mei and A. Hime, Phys. Rev. D 73, 053004 (2006)
[35] G. Mention, T. Lasserre, D. Motta, hep-ex/arXiv:0704.0498
[36] G. Bellini *et al.* arXiv:1003.0284
[37] Y. Suzuki, hep-ex/0110005
[38] J. G. Learned, S. T. Dye, S. Pakvasa, arXiv:0810.4975v1
[39] F. Montovani, L. Carmigniani, G. Fiorentini, M. Lissia, Phys. Rev. D 69 013001 (2004)
[40] G. Fiorentini, T. Lasserre, M. Lissia, B. Ricci and S. Schnert, Phys. Lett. B 558 (2003)
[41] J.M. Herndon and D.A. Edgerley, arXiv:hep-ph/0501216
[42] L. A. Currie, Analytical Chermistry 40 (1968) 586
[43] G. L. Fogli, E. Lisi, A. Palazzo, and A. M. Rotunno, arXiv:physics/0608025
[44] L. Oberauer, F. von Feilitzsch, W. Potzel, Nucl. Phys. B (Proc. Suppl.) 138 (2005) 108
[45] Petresa Canada, Linear Alkylbenzene, www.petresa.ca
[46] http://www.awa.tohoku.ac.jp/AAP2010/hapd.pdf
[47] A. Bernstein, T. West, and V. Gupta, Science and Global Security, Volume 9, pp. 235- 255, 2001 Taylor & Francis.